Journal of Physiology (1993), **462**, *pp.* 373–392
With 8 figures
Printed in Great Britain

HETEROGENEITY OF SYNAPTIC GLUTAMATE RECEPTORS ON CA3 STRATUM RADIATUM INTERNEURONES OF RAT HIPPOCAMPUS

BY CHRIS J. McBAIN* AND RAYMOND DINGLEDINE†

From the Department of Pharmacology, University of North Carolina, Chapel Hill, NC 27599, USA

(*Received 5 May 1992*)

SUMMARY

1. Whole-cell recordings were made from interneurones located within CA3 stratum radiatum of neonate rat hippocampal slices. All experiments were performed in the continued presence of tetrodotoxin (1 μM) and bicuculline (5 μM) to permit the isolation of spontaneous miniature excitatory synaptic currents (mEPSCs).

2. Two distinct populations of interneurones were identified based on current–voltage relations of kainate and the kinetic properties of spontaneous mEPSCs. These cell types were classified as type I and type II interneurones.

3. The *I–V* relation of kainate in type I cells was linear or modestly outwardly rectifying. Currents reversed polarity close to 0 mV. The kainate *I–V* relationship in type II interneurones was strongly inwardly rectifying with little or no outward current passed at potentials up to +50 mV.

4. Spontaneous mEPSCs were observed at a low frequency. At −70 mV mEPSCs received by type I interneurones had fast rise times (~ 1 ms) and decay time constants (~ 5 ms) and were mediated by α-amino-3-hydroxy-5-methylisoxazole-4-propionic acid (AMPA) receptors. Miniature EPSCs on type I interneurones reversed polarity at ~ 0 mV. At +50 mV the kinetics of the mEPSCs on type I interneurones were slowed and comprised both AMPA and *N*-methyl-D-aspartate (NMDA) receptor-mediated components as revealed by their sensitivity to 6-cyano-7-nitroquinoxaline-2,3-dione (CNQX) and D-2-amino-5-phosphonovaleric acid (D-APV).

5. The kinetics of spontaneous mEPSCs on type II cells were slower than their type I counterparts at −70 mV. Spontaneous mEPSCs received by type II interneurones showed extreme inward rectification with no cells possessing fast events at +50 mV. In a few cells slowly rising and slowly falling spontaneous mEPSCs were observed at positive holding potentials. These events were abolished by D-APV and were therefore mediated solely by NMDA receptor activation.

6. Type I or type II interneurones filled with Lucifer Yellow or biocytin possessed similar morphologies. Both cell types were typically large triangular cells with three

* Present address and address for correspondence: National Institutes of Health, Building 49, Room 5A72, Bethesda, MD 20892, USA.

† Present address: Department of Pharmacology, Rollins Building, Emory University School of Medicine, Atlanta, GA 30322, USA.

MS 1341

to six branching dendrites often possessing varicosities. The dendrites of these interneurones arborized throughout strata radiatum, pyramidale, oriens and the molecular layer of the dentate gyrus.

7. In the majority of interneurones (both type I and II) the rise times of individual mEPSCs were correlated with their half-width and decay time constant, suggesting that the shape of the mEPSC is in part determined by the dendritic origin of the synaptic input.

8. The interneurone population within CA3 stratum radiatum is thus heterogeneous with respect to glutamate receptor expression. The inward or outward rectification observed in the two cell types for both exogenous kainate and excitatory synaptic receptors is likely to be due to expression of different glutamate receptor subunits.

INTRODUCTION

Hippocampal interneurones located both in CA3 stratum radiatum and the oriens/alveus ramify extensively throughout the cell body and dendritic layers of stratum pyramidale (Lorente de Nò, 1934; Ramon y Cajal, 1968). Virtually all these cells stain for glutamate decarboxylase (GAD), the synthesizing enzyme for the inhibitory neurotransmitter γ-aminobutyric acid (GABA) (Ribak, Vaughn & Saito, 1978; Ribak, Vaughn & Barber, 1981; Somogyi, Smith, Nunzi, Gorio, Takagi & Wu, 1983; Frotscher, Leranth, Lubbers & Oertel, 1984) and are presumed to be inhibitory in nature. It is likely that these interneurones are responsible for the barrage of inhibitory input received by CA3 pyramidal neurones (Miles & Wong, 1984, 1987; Miles 1991; McBain & Dingledine, 1992). This inhibition appears to be sufficiently strong to limit the spread of synaptic excitation within the hippocampus (Miles & Wong, 1987; Traub, Miles, Wong, Schulman & Schneiderman, 1987; Swann, Brady & Martin, 1989). In return CA3 interneurones receive excitatory input from recurrent collaterals of pyramidal cells (Miles & Wong, 1984), mossy fibres of dentate granule cells (Frotscher, 1985) and extrinsic hippocampal afferents (Andersen, 1975; Loy, 1980; Buszaki & Eidelberg, 1982; Frotscher & Zimmer, 1983; Frotscher *et al.* 1984). Anatomical studies indicate that these excitatory synapses impinge onto the soma and proximal dendrites of hippocampal inhibitory cells (Frotscher, 1985; Schwartzkroin & Kunkel, 1985; Seress & Ribak, 1985; Kisvarday, Martin, Freund, Magloczky, Whitteridge & Somogyi, 1986; Lang & Frotscher, 1990). Unlike excitatory synapses on pyramidal neurones, excitatory synapses on most hippocampal interneurones are not onto dendritic spines, at least in the guinea-pig (Frotscher, 1985; Schwartzkroin & Kunkel, 1985; Seress & Ribak, 1985). To date most studies of hippocampal interneurones have been performed on a mixed population of cells derived from the alveus, stratum oriens and stratum radiatum. A detailed study of the interneurones located solely within stratum radiatum has not been reported.

It is generally accepted that glutamate is the major excitatory neurotransmitter released onto interneurones (Storm-Mathisen, Leknes, Bore, Vaaland, Edminson, Haug & Ottersen, 1983). Little is known, however, about the identity of the excitatory receptors on CA3 stratum radiatum interneurones (see Miles, 1991). Evoked excitatory postsynaptic currents (EPSCs) on guinea-pig interneurones of

CA3 stratum radiatum and alveus (Miles, 1991) appear to be larger and faster when compared to those events observed on CA3 pyramidal neurones (Miles & Wong, 1984). This observation was attributed to the different cable properties of the two cell types (Miles, 1991).

To date four genes have been identified that encode AMPA receptor subunits (Boulter, Hollmann, O'Shea-Greenfield, Hartley, Deneris, Maron & Heinemann, 1990; Keinanen, Wisden, Sommer, Werner, Herb, Verdoorn, Sakmann & Seeburg, 1990; Nakanishi, Shneider & Axel 1990; Sakimura, Bujo, Kushiya, Araki, Yamazaki, Meguro, Warashina, Numa & Mashina, 1990), each of which is expressed in at least two splice variants (Sommer, Keinanen, Verdoorn, Wisden, Burnashev, Herb, Kohler, Tagaki, Sakmann & Seeburg, 1990). Glutamate receptors expressed in *Xenopus* oocytes or mammalian cell lines from combinations of GluR1, GluR3 and GluR4 exhibit strong inward rectification, whereas incorporation of the GluR2 subunit causes the kainate current–voltage (*I–V*) relation to become linear or outwardly rectifying (Boulter *et al.* 1990; Nakanishi *et al.* 1990). It is likely that the biophysical and pharmacological properties of the native non-NMDA receptors on hippocampal cells will also depend on the particular subunit combinations expressed. The distribution of AMPA receptor subunit mRNAs shows marked regional heterogeneity throughout the developing hippocampus (Monyer, Seeburg & Wisden, 1991; Werner, Voigt, Keinanen, Wisden & Seeburg, 1991). Most non-NMDA receptors studied in hippocampal neurones have an approximately linear *I–V* relationship (Mayer & Westbrook, 1987; Hestrin, Nicoll, Perkel & Sah, 1990; Sah, Hestrin & Nicoll, 1990; McBain & Dingledine, 1992). In cultured hippocampal neurones, however, an unidentified cell type has been described which showed a sigmoidal kainate *I–V* relationship (Iino, Ozawa & Tsuzuki, 1990; Ozawa, Iino & Tsuzuki, 1991).

We have made whole-cell voltage clamp recordings from neurones with non-pyramidal morphology that are located in stratum radiatum of CA3 of immature rat hippocampal slices. We have broadly characterized these interneurones into two major populations based on EPSC kinetics and responses to the AMPA receptor agonist, kainate. A preliminary report of some of these findings has been made (McBain & Dingledine, 1991).

METHODS

Rat hippocampal slices (300 μm thick) from Sprague–Dawley rats killed by decapitation were prepared as described previously (McBain & Dingledine, 1992). Most recordings were made from 8- to 15-day-old rats, although a few cells were recorded from earlier ages. Slices were held in a submerged chamber and perfused at a rate of 1–2 ml/min with the following medium (mM): NaCl, 130; $NaHCO_3$, 24; KCl, 3·5; NaH_2PO_4, 1·25; $CaCl_2.2H_2O$, 1·5; $MgSO_4.7H_2O$, 1·5; glucose, 10; saturated with 95% O_2–5% CO_2 (pH 7·4, 307 mosmol/l) at 22–25 °C. All drugs were bath applied in known concentrations by direct addition to the perfusate. Unless stated otherwise, all experiments were performed in the presence of tetrodotoxin (1 μM) and bicuculline methobromide (5 μM) to eliminate EPSCs triggered by action potentials and most inhibitory synaptic currents respectively.

Tight-seal (> 1 GΩ) whole-cell recordings (Hamill, Marty, Neher, Sakmann & Sigworth, 1981; Edwards, Konnerth, Sakmann & Takahashi, 1989) were obtained from the cell bodies of sixty-one interneurones in stratum radiatum of CA3. Patch electrodes were fabricated from borosilicate glass and were typically not fire-polished. They had resistances of 3–8 MΩ when filled with (mM):

caesium methanesulphonate, 140; Hepes, 10; $MgCl_2$, 2 (buffered to pH 7·3 with CsOH, 275 mosmol/l). Lucifer Yellow (0·3%) or biocytin (0·7%) was usually included in the recording electrode to allow observation of cell morphology. Electrodes were typically coated with Sylgard (Dow Corning Corporation). The electrode was positioned under visual control within the stratum radiatum of CA3; individual cells were visualized using an Hoffman objective (overall magnification 600×). Interneurones were usually located in CA3b. Breakthrough to the whole-cell mode was performed under current clamp in order to provide an initial evaluation of the passive membrane and action potential properties of the interneurone. Cells possessing an initial resting potential more negative than −50 mV (mean, −60 ± 1·5 mV; $n = 42$) and overshooting action potentials were accepted. The dialysis of the neurone by Cs^+ usually resulted in the cell stabilizing at a more positive potential. In addition cells that fired action potentials on the anode break were discarded. Interneurones were then voltage clamped at −70 mV unless stated otherwise in the text. CA3 stratum radiatum interneurones had input resistances ranging from 100–1000 MΩ (mean ± S.E.M., 490 ± 30 MΩ; $n = 42$) at this holding potential. The measured membrane capacitance was 43 ± 3·7 pF ($n = 27$). Occasionally glial cells were encountered, identified as such by their high resting potential (> −70 mV), lower input resistance (~ 200 MΩ), and absence of spikes.

All currents were recorded with an Axopatch-1D amplifier (Axon Instruments, USA); records were filtered at 2 or 3 kHz (−3 dB) and digitized at 3–30 kHz on a 80486 computer. Signals were also stored on FM tape (5 kHz bandwidth) for off-line analysis. The steady-state *I–V* relation of bath-applied kainate was obtained by measuring the current at the end of 250–1000 ms voltage steps applied in −10 mV increments at 10 s intervals. A holding potential of +50 mV was selected for these studies to inactivate most voltage-dependent currents. *I–V* relations were obtained prior to, during addition and following removal of kainate. The mean of control and recovery *I–V* relations was then subtracted from that in kainate. The kainate conductance ratio was determined by dividing the slope conductance of the *I–V* relation measured between +50 and +40 mV by the slope conductance measured between −50 and −40 mV.

Individual mEPSCs were identified visually and accepted for analysis if the mean current associated with the event was significantly different from that of an equivalent length of pre-event baseline. The 10–90% rise time was calculated by linear regression over the appropriate data points. Measurements of the decay time constant of synaptic currents represent the mean of at least fifteen individual events from each cell and were fitted by the sum of one or two exponential components (simplex algorithm, least-squares criteria). In some experiments to increase the spontaneous mEPSC frequency the bathing solution was made hyperosmotic by the addition of 100 mosmol/l mannitol (Bekkers & Stevens, 1989; McBain & Dingledine, 1992).

For measurements of membrane and dendritic time constants, electrotonic pulses (100 pA, duration 100–1000 ms) were delivered at 0·5–1 Hz in current clamp mode. The voltage deflection was digitized at 30 kHz. The electrotonic length was calculated from the equation:

$$L = \pi[((\tau_m/\tau_o)-1)^{-1/2}]$$

where L is the electrotonic length, and τ_m and τ_o the membrane and fast dendritic time constants respectively (Rall, 1969; Johnston & Brown, 1983).

The series resistance typically ranged from 10 to 30 MΩ (mean, 25 ± 1·4 MΩ, from a sample of twenty-seven interneurones). The amplitude of the excitatory synaptic currents was never in excess of 60 pA, thus a series resistance of 25 MΩ would result in a DC series resistance error of no greater than 1·5 mV. Membrane potentials were not corrected for these errors. In contrast, the large currents induced by kainate at potentials more negative than −60 mV can result in significant series resistance error. This probably accounts for the bending of some *I–V* relations between −60 and −80 mV (e.g. Fig. 2*A*), which we consider artifactual. No combination of glutamate receptor subunits expressed in oocytes from cDNAs displays this form of rectification.

All data are represented as the means ± standard error of the mean. Where appropriate an unpaired Students *t* test was performed.

Drugs used were tetrodotoxin (TTX, Sigma, St Louis, MO, USA), bicuculline methobromide (Sigma), D-2-amino-5-phosphonovaleric acid (D-APV, Cambridge Research Biochemical, Cambridge, MA, USA), 6-cyano-7-nitro-quinoxaline-2,3-dione (CNQX, Tocris Neuramin, Essex), Lucifer Yellow dipotassium salt (Sigma), kainic acid (Sigma) and biocytin (Sigma).

RESULTS

Passive membrane properties

Whole-cell recordings were made from a total of sixty-one stratum radiatum interneurones. Based on pharmacological properties and the kinetic properties of the spontaneous miniature EPSCs, interneurones could be classed into two cell types which we will subsequently refer to as type I and type II (see below). Recordings were made from a total of forty-seven type I and fourteen type II interneurones. The lower number of type II interneurones encountered probably reflects their low density rather than recording difficulties, since the quality of recordings made from both cell types were comparable. The resting membrane potential and input resistances of both cell types were not significantly different from each other (Table 1) and were comparable to data obtained from CA3 pyramidal neurones recorded under similar conditions (McBain & Dingledine, 1992). The membrane *I–V* relation in the absence of agonists was essentially linear for both type I and type II interneurones (not shown). An accurate estimation of the electrotonic length was obtained from seven type I and two type II interneurones. Type I interneurones possessed a mean electrotonic length of $0{\cdot}6 \pm 0{\cdot}06$. The two type II interneurones had electrotonic lengths of 0·6 and 0·2. These data are also comparable to the electrotonic length of CA3 pyramidal neurones from animals of the same age range (0·52, McBain & Dingledine, 1992).

Type I interneurones

The classification of these cells into two main types was determined by their different *I–V* relations to kainate together with the *I–V* properties of their spontaneous mEPSCs.

Kainate I–V relation

At negative holding potentials all cells tested responded to kainate (30–100 μm) with a non-desensitizing inward current. The current–voltage relationship of a type I interneurone to kainate is illustrated in Fig. 1*A*. The kainate current reversed polarity at $+4{\cdot}3 \pm 0{\cdot}8$ mV ($n = 40$ neurones). Many cells demonstrated modest outward rectification. The ratio of slope conductance measured at positive and negative potentials permits comparison of the degree of rectification among a population of cells. A conductance ratio of unity occurs for a linear *I–V* relation, whereas a ratio greater than unity is indicative of an outwardly rectifying current and a ratio of less than one indicates inward rectification. The mean conductance ratio of kainate currents in type I cells was $1{\cdot}25 \pm 0{\cdot}06$, measured at +45 and −45 mV.

Kinetics of spontaneous mEPSCs

In the presence of tetrodotoxin (1 μM) and bicuculline (5 μM) mEPSCs were detected. Although both cell types received mEPSCs at a low frequency (range, 0·1–5 Hz; mean, $1{\cdot}4 \pm 0{\cdot}4$ Hz; $n = 10$ cells in the absence of mannitol) the properties of these mEPSCs markedly differed in the two cell types. Miniature EPSCs received by type I interneurones were typically larger at −70 mV and possessed faster kinetics than those received by type II interneurones (Table 1).

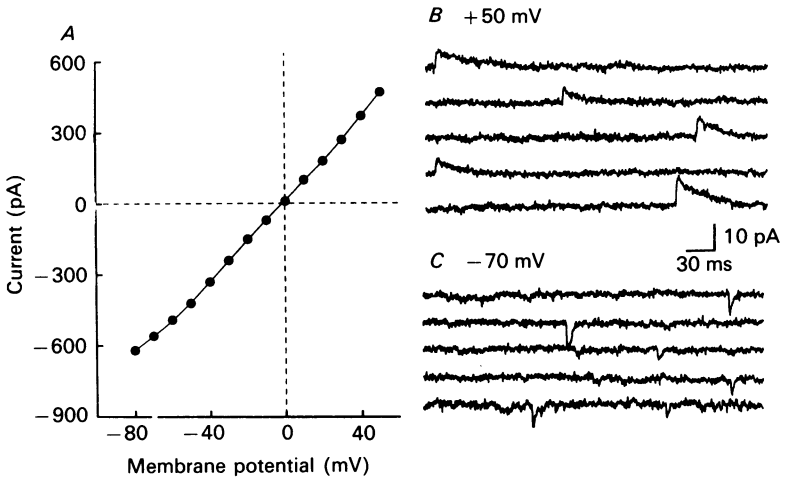

Fig. 1. *I–V* relation of kainate and spontaneous mEPSCs in a type I interneurone. *A*, modest outward rectification of the *I–V* relation of 100 μM kainate. In this interneurone the ratio of slope conductance measured at +45 and −45 mV was 1·2. Kainate current reversed polarity at 0 mV. *B* and *C*, spontaneous mEPSCs recorded in the presence of TTX and bicuculline. At a holding potential of −70 mV EPSCs were inward-going and clearly discernible from the baseline noise. In this interneurone the mean amplitude, rise time and decay time constant (τ_{decay}) were 8·5 pA, 1·4 and 3·2 ms respectively. Holding the cell at +50 mV reversed the polarity of the EPSC. At +50 mV the EPSC was dominated by a large slowly rising and decaying second component. The mean amplitude, rise time and decay time constant of the EPSCs at +50 mV were 18 pA, 2·1 ms and 27 ms respectively.

TABLE 1. A comparison of the resting membrane properties and spontaneous mEPSCs of types I and II interneurones and CA3 pyramidal neurones

	Type I	Type II	Pyramidal neurone†
Resting potential (mV)	−59±1·5 (n = 47)	−65±2·8 (n = 14)	−59±2·2 (n = 39)
Input resistance (MΩ)	502±29	410±53	411±42
Membrane τ_m (ms)	45±3·6 (n = 14)	37±12 (n = 3)	48±5·2 (n = 23)
Electrotonic length	0·60±0·06 (n = 8)	0·6 and 0·22	0·52±0·03 (n = 6)
Miniature EPSC (V_{hold} = −70 mV)			
Amplitude (pA)	18±2·5 (n = 25)	11±2·0 (n = 10)*	18±2·3 (n = 28)
Rise time (ms)	1·2±0·1	2·8±0·5*	2·5±0·2*
τ_{decay} (ms)	5·5±0·4	13·8±2·9*	16±1·6*
Miniature EPSC (V_{hold} = +50 mV)			
Amplitude (pA)	16·4±1·5 (n = 15)	16·7±2·0 (n = 3)‡	25±5·7 (n = 11)
Rise time (ms)	4·4±0·6	7·9±1·8	7·2±1·1*
τ_{decay} (ms)	27±5·0	52·2±11·6	77±18*

Numbers in parentheses represent the number of cells used.
* Significantly different from type I interneurones (P = 0·05).
† Data taken from McBain & Dingledine (1992).
‡ Only three of fourteen cells possessed EPSCs at positive potentials, see text for details.

To investigate the *I–V* relation of spontaneous mEPSCs, at least fifteen (usually 50–200) events were captured and aligned on the foot of each mEPSC and digitally averaged. Measurements were made at two holding potentials, −70 and +50 mV.

Miniature EPSCs in type I cells were detected at both potentials, as shown by the cell in Fig. 1*B* and *C*. At a holding potential of −70 mV, mEPSC rise times ranged between 0·5–2·5 ms (Table 1) and the mean half-width was 5·8 ± 0·4 ms ($n = 25$ cells). The decay phase of mEPSCs at −70 mV was described by a single exponential with

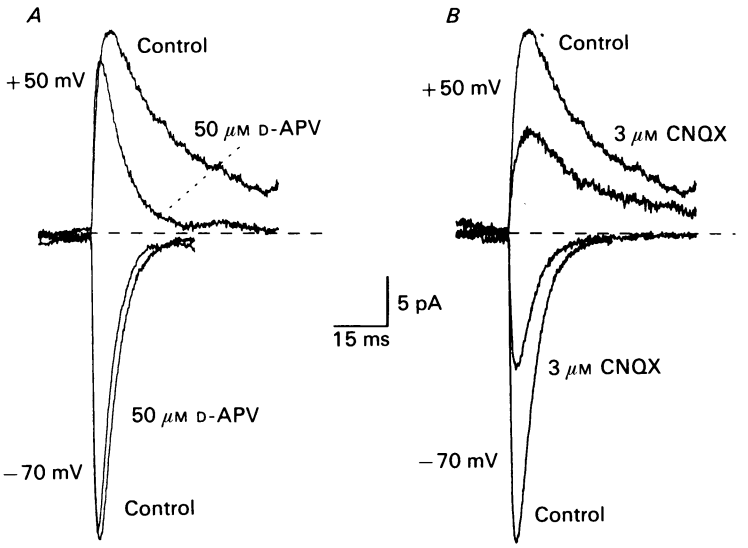

Fig. 2. NMDA and AMPA receptor components of spontaneous mEPSCs in type I interneurones. *A* and *B*, a single neurone voltage clamped at −70 and +50 mV demonstrates that spontaneous mEPSCs on type I interneurones comprise both NMDA and non-NMDA receptor-mediated components. The slice is perfused with TTX (1 μM) and bicuculline (5 μM). Each trace is the average of 120 events at −70 mV and 50 events at +50 mV, aligned at the foot of the rising phase. *A*, the decay time constants of the averaged control spontaneous mEPSC at −70 and +50 mV were best described by single exponentials with time constants 5·1 and 20 ms respectively. D-APV (50 μM) did not alter the decay time constant at −70 mV (4·1 ms). Following addition of D-APV, events at +50 mV were described by a single exponential with decay time constant of 6·7 ms. The peak amplitude of the EPSC at +50 mV was reduced from 26 pA in control to 23 pA following addition of D-APV. The rise time of the EPSC was also reduced at +50 mV by D-APV, from 2·6 to 1·9 ms. *B*, in the same neurone voltage clamped at −70 mV, addition of CNQX (3 μM) following wash-out of D-APV reduced the peak amplitude of the mean event (35 pA in control *versus* 18 pA in CNQX) and caused a slight reduction in mean rise time (1·8 *versus* 1·4 ms) and decay time constant (5·2 *versus* 4·8 ms). At +50 mV addition of CNQX reduced the peak amplitude (24 *versus* 12 pA), but increased the decay time constant (17 *versus* 34 ms) and rise time (2·6 *versus* 4·6 ms).

time constant (τ_{decay}) of ~ 6 ms (Table 1). At +50 mV, mEPSCs in all type I interneurones were outward and their kinetics were markedly slowed. At this holding potential mEPSCs were dominated by a prominent slowly rising and decaying component, which is obvious in the cell shown in Fig. 1*B*. The decay phase of this slow component was described by a single exponential of ~ 27 ms (Table 1). The mean half-width of the events at +50 mV was 27 ± 4·7 ms. In all seventeen cells examined, the late slow phase present at +50 mV was absent at −70 mV (Fig. 2*C*), consistent with the voltage-dependent block of the NMDA receptor by magnesium ions (Mayer, Westbrook & Guthrie, 1984; Nowak, Bregestovski, Ascher, Herbet &

Prochiantz, 1984). Assuming that the I–V relation of the mEPSC was linear, the mean mEPSC amplitudes of −18 and +16 pA, observed at holding potentials of −70 and +50 mV respectively (Table 1), predicts a mean reversal potential of +2·1 mV. In the same cells the reversal potential of kainate current was similar, +4·3 mV.

TABLE 2. Effects of CNQX and D-APV on the kinetics of mEPSCs of type I interneurones

	Control	D-APV (50 μM)	CNQX (3 μM)
$V_{hold} = -70$ mV			
Rise time (ms)	1·3±0·2 ($n = 6$)	0·8±0·2	1·2±0·2 ($n = 4$)
τ_{decay} (ms)	4·1±0·07	4·1±0·1	4·6±0·5
$V_{hold} = +50$ mV			
Rise time (ms)	4·3±0·2 ($n = 6$)	1·8±0·5*	7·8±0·6 ($n = 4$)*
τ_{decay} (ms)	27·3±5·3	7·3±1·9*	58±1·7

Numbers in parentheses are the number of cells in study.
* Significantly different from control ($P = 0·05$).

Pharmacology of mEPSC

Figure 2 shows the effects of both the AMPA receptor antagonist, CNQX and the NMDA receptor antagonist, D-APV on the kinetics of spontaneous mEPSCs recorded from a type I interneurone. In all six interneurones tested D-APV was without effect on the holding current of the cell (cf. Sah, Hestrin & Nicoll, 1989). Figure 2*A* illustrates averaged mEPSCs recorded at −70 and +50 mV following the addition of D-APV. D-APV (50 μM) had no significant effect on spontaneous mEPSCs at −70 mV but at +50 mV the slow component of the mEPSC was absent and the rise time was marginally reduced. The time constant of decay of the mEPSC in D-APV at both −70 and +50 mV was best described by a single exponential. These values were not significantly different (Table 2), suggesting that the decay time constant of the non-NMDA receptor component remaining in D-APV was not voltage dependent. This voltage independence is similar to that obtained for spontaneous mEPSCs on immature CA3 pyramidal neurones (McBain & Dingledine, 1992) and for Schaffer–commissural synapses onto CA1 pyramidal cells (Hestrin *et al.* 1990), but not for the mossy fibre synapses onto CA3 pyramidal cells (Brown & Johnston, 1983).

At a holding potential of −70 mV the addition of CNQX (3 μM) attenuated the mean amplitude of the events without affecting the kinetics (Fig. 2 and Table 2). At +50 mV, however, the mEPSC remaining in CNQX had a slower rate of rise and prolonged decay (Fig. 2*B* and Table 2), due presumably to the predominance of the NMDA receptor component. The decay time constant remaining in CNQX was fitted by a single exponential that was significantly slower than control (Table 2).

These results are qualitatively similar to those obtained from CA3 pyramidal neurones (McBain & Dingledine, 1992) and cultured hippocampal neurones (Bekkers & Stevens, 1989) and indicate that individual miniature mEPSCs in CA3 type I interneurones could display both NMDA and non-NMDA postsynaptic receptor components. In contrast to the fast mEPSCs observed on CA3 pyramidal neurones (McBain & Dingledine, 1992), D-APV did not reduce the mean amplitude of interneurone mEPSCs at −70 mV.

Type II interneurones

Kainate I–V relation

Like type I interneurones, type II cells responded to kainate (100 μM) with a sustained inward current. In contrast to type I interneurones, however, the kainate response of all type II interneurones displayed strong inward rectification at positive potentials (Fig. 3*A*). In this study *I–V* relations were considered inwardly rectifying if the conductance ratio measured at +45 and −45 mV was less than 0·6. In six of these cells the slope conductance ratio was less than 0·3, and in five cells no outward current was observed at potentials more positive than 0 mV. The mean conductance ratio of type II interneurones was 0·24 ± 0·07 (n = 14 cells).

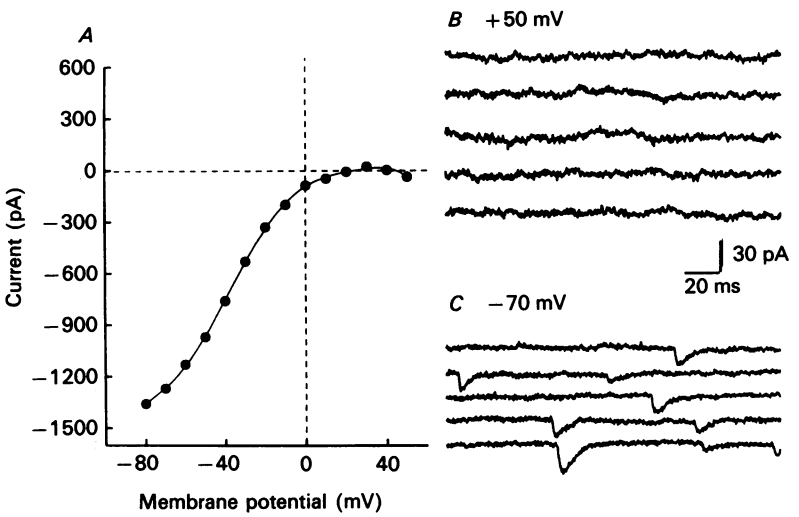

Fig. 3. Typical *I–V* relation of kainate and spontaneous mEPSCs in a type II interneurone. *A*, strong inward rectification of the kainate *I–V* relation. In this cell no outward current was observed at positive potentials. *B*, at a holding potential of +50 mV no detectable mEPSCs were observed. *C*, at a holding potential of −70 mV the mean amplitude, rise time and decay time constant of spontaneous mEPSCs were 15 pA, 4·5 ms and 15 ms respectively.

Voltage dependence of mEPSCs

Spontaneous mEPSCs on type II interneurones showed markedly different properties from those observed on type I interneurones. First, as illustrated by the cell in Fig. 3*B*, in all ten type II interneurones examined no fast-rising spontaneous mEPSCs were observed at +50 mV. Miniature EPSCs in these cells were strongly inwardly rectifying as was the response to kainate. Due to the small amplitude of these events ($\sim$ 10 pA at a holding potential of −70 mV) and low frequency it was not possible to determine the membrane potential at which these events disappeared. Second, at a holding potential of −70 mV mEPSCs were generally smaller in amplitude and possessed slower kinetics than type I mEPSCs. At −70 mV the rise time of the mEPSCs ranged between 1·1 and 4·7 ms and the half-width was

15·4 ± 3·2 ms ($n = 10$ cells). At this holding potential the decay phase of the EPSC was described by a single exponential of ~ 15 ms.

The kinetic properties of mEPSCs on type I and II interneurones are compared in Table 1. The *I–V* relations of spontaneous mEPSCs observed on both type I and type II interneurones were in close agreement with the *I–V* relations to kainate in the same cell.

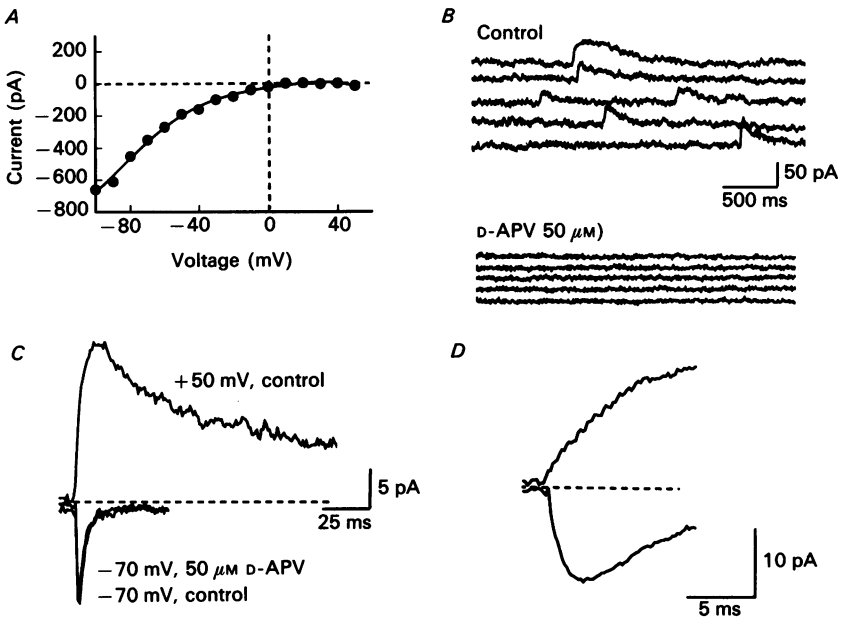

Fig. 4. Pure NMDA receptor-mediated mEPSCs in a type II interneurone. *A*, strong inward rectification of the kainate *I–V* relation in one of the three type II interneurones possessing EPSCs at positive holding potentials. *B*, in the same cell spontaneous mEPSCs were captured at +50 mV. This cell displayed large (mean, 21 pA) long-lasting mEPSCs, with mean rise time of 12 ms and the decay time constant of 74 ms. Following the addition of D-APV no events were observed at +50 mV. *C*, averaged mEPSCs at −70 mV ($n = 150$ events) and +50 mV ($n = 65$). D-APV (50 μM) was without effect on the rise time, amplitude and decay time constant of the averaged EPSC at −70 mV. No events were detected at +50 mV in D-APV. *D*, a comparison of the rising phases of the EPSCs in *B* shown on a faster time base demonstrates the lack of the fast EPSC component (presumably mediated by AMPA receptors) in the events recorded at +50 mV. At the time when the fast EPSC (lower trace) has attained its maximum amplitude (1·2 ms) the EPSC at +50 mV (upper trace) has reached less than 40% of its peak amplitude.

Pharmacology of mEPSCs

As stated previously the majority of type II interneurones displayed mEPSCs *only* at negative holding potentials. In three neurones held at +50 mV, however, slowly rising and slowly falling mEPSCs were observed. Figure 4 shows the kainate *I–V* relation of one such type II interneurone and the mean spontaneous mEPSCs obtained from this cell at −70 and +50 mV. The decay time constant of the averaged mEPSC at +50 mV followed a single exponential of 74 ms (Fig. 4*C*). D-APV had no effect on mEPSC kinetics at a holding potential of −70 mV, but

abolished events at +50 mV (Fig. 4*B* and *C*). D-APV also had no effect on the amplitude (mean, 11·4 pA) or the frequency (0·83 Hz) of mEPSCs at negative potentials. The time scale is expanded in Fig. 4*D* to compare the rise times of mEPSCs at −70 and +50 mV. The fast mEPSC has decayed by ~ 80% before the slow mEPSC at +50 mV has reached its peak.

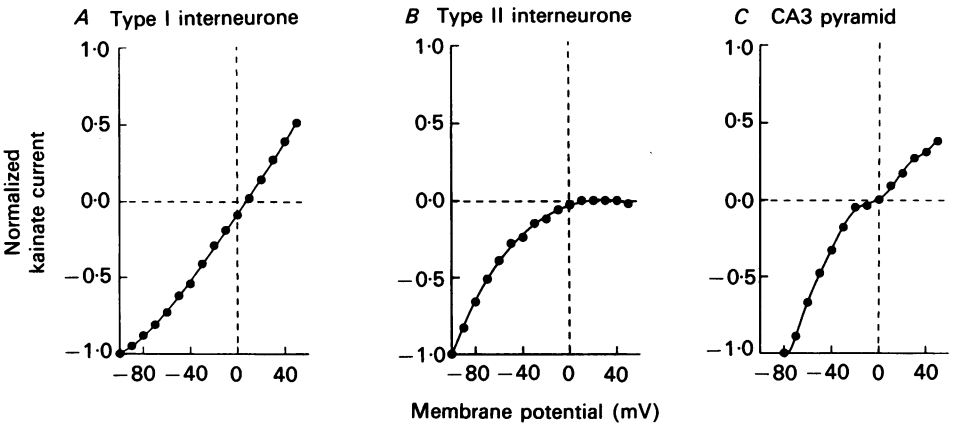

Fig. 5. *I–V* relations of kainate in types I and II interneurones and a CA3 pyramidal neurone. *I–V* relations are normalized to the current amplitude at −100 mV (−80 mV for the pyramidal neurone) for comparisons among the three cell types. In contrast to the stereotyped shape of the *I–V* relation in type I and type II interneurones, the CA3 pyramidal neurone illustrates a more complex *I–V* relation often observed in these cells.

These results suggest that in type II interneurones spontaneous mEPSCs observed at +50 mV may be mediated solely by NMDA receptor activation.The absence of D-APV-insensitive EPSCs at +50 mV (Fig. 4*B*) is consistent with inward rectification of AMPA receptors activated by kainate in these cells (Fig. 4*A*). These data also suggest that NMDA and non-NMDA receptors are not necessarily co-localized at the same synapses since the frequency of fast events at −70 mV was much higher than that of slow events at +50 mV. It should be stressed, however, that the majority of type II interneurones did not possess any mEPSCs at +50 mV, suggesting that synapses on these interneurones are devoid of NMDA receptors but instead possess AMPA receptors capable of passing only inward current. Although we have not tested the response of type II interneurones to NMDA, the D-APV-sensitive rumbling of membrane current at +50 mV, indicative in CA3 pyramidal cells of tonic NMDA receptor activation (McBain & Dingledine, 1992), is not prominent in these cells.

A comparison with CA3 pyramidal neurone I–V properties

It is interesting to compare the kainate *I–V* relations obtained from type I and II interneurones with those from CA3 pyramidal neurones. Figure 5 shows *I–V* relations from the three cell types. In each cell, currents are expressed relative to the current measured at −100 or −80 mV. Whereas type I and II interneurones usually displayed either outwardly or inwardly rectifying *I–V* relations as described above,

CA3 pyramidal neurones exhibited a variety of degrees of rectification. The *I–V* relation of most pyramidal cells was approximately linear, but some neurones had *I–V* relations that showed a distinct break in the curve suggestive of mixed inward and outward rectification, as shown in Fig. 5*C*. The kainate conductance ratio of

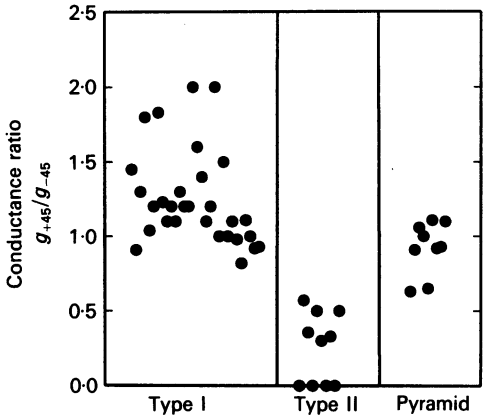

Fig. 6. The conductance ratios of the kainate *I–V* relation obtained from types I and II interneurones and CA3 pyramidal neurones. The ratio of slope conductance measured at +45 and −45 mV (g_{+45}/g_{-45}) is plotted for all cells studied. Type I interneurones all had rectification indices close to or greater than unity (mean, 1·25±0·06; $n = 30$). The majority of these cells displayed outwardly rectifying curves as depicted in Figs 2 and 6*A*. All type II interneurones had a rectification index less than one (mean, 0·24±0·07; $n = 14$). In contrast the mean rectification index of CA3 pyramidal cells was close to unity (mean, 0·92±0·02; $n = 10$).

pyramidal cells was typically intermediate between that of types I and II interneurones, as shown in the scatter plot of all neurones studied in Fig. 6. A simple interpretation of these *I–V* relations is that type II interneurones may express AMPA receptors that lack the GluR2(R) subunit. The more complex *I–V* relation of some CA3 pyramidal neurones possibly results from the activation of a mixed population of inwardly and outwardly rectifying receptors, the relative proportion of which varies from cell to cell.

Block of kainate currents by CNQX

In all nine type I interneurones tested, the response to 100 μM kainate could be reversibly antagonized by the AMPA receptor antagonist CNQX. At a concentration of 3 μM, CNQX blocked 76±8·1% ($n = 9$) of the current (range of block, 31–100%) at a membrane potential of −100 mV. The effect of CNQX was not voltage dependent since kainate currents were reduced by 76±9·9% at +50 mV.

We recorded the effects of CNQX on two type II interneurones possessing some outward current at positive holding potentials. In both cases the block of the kainate response by CNQX was greater at negative than at positive membrane potentials. At membrane potentials of −80 and +50 mV the kainate currents in both cells were blocked by 75 and 36% respectively.

We have previously described that CNQX (3 μM) directly depolarizes a small population of interneurones located in stratum radiatum of CA3 (McBain, Eaton, Brown & Dingledine, 1992). In this study this effect of CNQX was observed on only two type I and one type II interneurones.

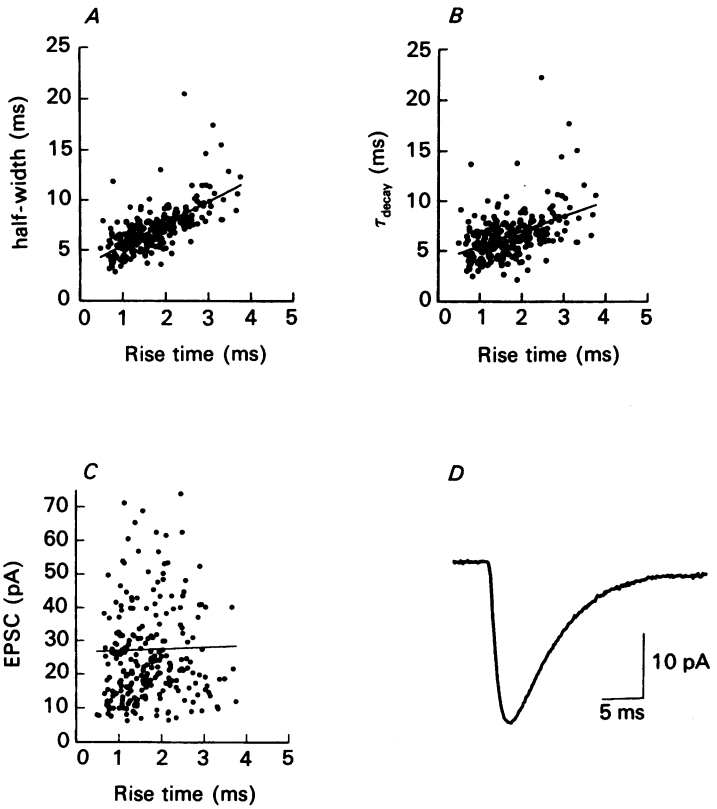

Fig. 7. Correlation between the shape indices of spontaneous EPSCs. Half-width (*A*), decay time constant (*B*) and peak amplitude (*C*) are plotted against the rise time for 268 EPSCs from a single type I interneurone clamped at −70 mV. A close correlation was found for the plot of the rise time against the half-width ($r = 0{\cdot}7$). A weak correlation was observed for the plots against decay time constant and peak amplitude ($r = 0{\cdot}4$ and $0{\cdot}2$ respectively). *D*, the averaged mEPSC obtained from this cell. The mean parameters were rise time = 1·7 ms, decay time constant (τ_{decay}) = 6·5 ms and peak amplitude = 27 pA. These data suggest that a correlation exists between the rise time and half-width and that the variety of EPSC shapes can be in part accounted for by dendritic filtering of the EPSC.

Electrotonic filtering of mEPSCs

Electrotonic filtering contributes to the shape and size of mEPSCs on CA3 pyramidal neurones (McBain & Dingledine, 1992). Dendritic filtering of mEPSCs is also marked in types I and II interneurones. Figure 7 shows a plot of the decay time constant, half-width and the peak amplitude as a function of the rise time from 268 individual mEPSCs recorded from a single type I interneurone. In ten of fourteen

neurones examined (both types I and II), these plots revealed a correlation between rise time and half-width suggesting that dendritic filtering of the synaptic input contributes substantially to the mEPSC shape (Rall, 1969). Figure 7*C* illustrates that the amplitude distribution of these mEPSCs is skewed as reported previously for

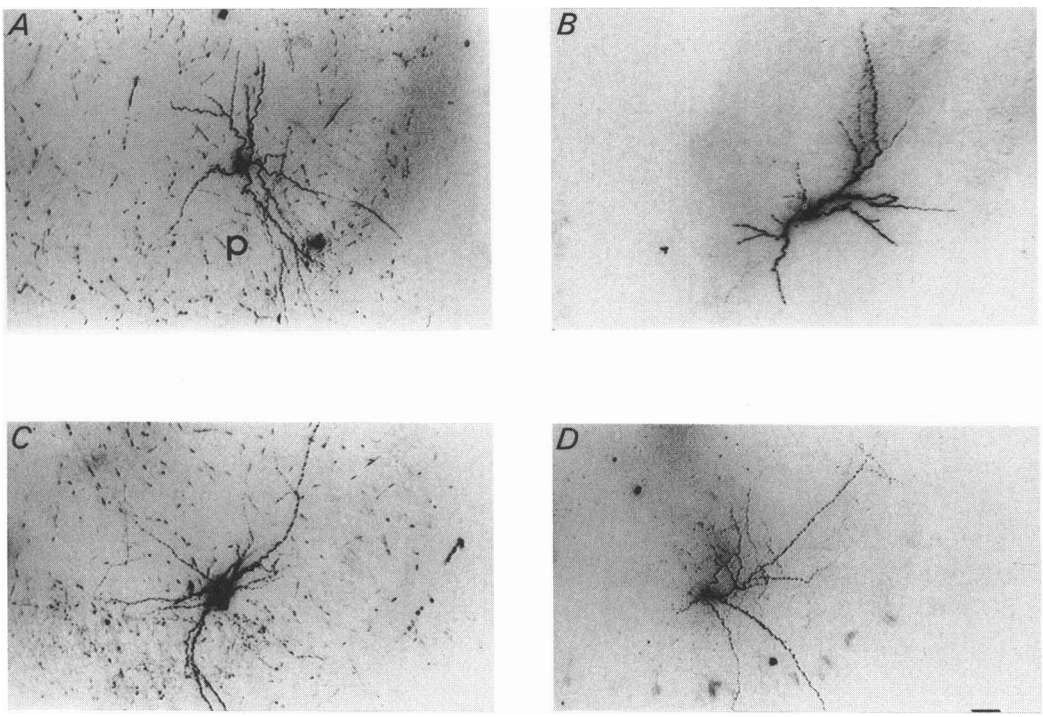

Fig. 8. Morphological properties of biocytin-labelled type I and type II stratum radiatum interneurones. Both type I (*A* and *B*) and type II (*C* and *D*) stratum radiatum interneurones share common morphologies. All panels of this figure show cells classified as non-pyramidal, located within stratum radiatum of CA3, stained with biocytin (0·7 % and serially reconstructed). All cells are shown in a similar orientation with respect to the CA3 pyramidal cell layer (marked 'p' in panel *A*). All interneurones possess large triangular cell bodies with radially oriented dendrites. The dendrites of these cells branch often and project into stratum pyramidale, stratum oriens and the alveus together with terminations within stratum radiatum. The dendrites of type I and type II interneurones often possessed varicosities (*B*, *C* and *D*). *C* and *D*, cells classified physiologically as type II interneurones possessed similar morphologies to type I interneurones. In these two cells the dendritic projections were laminar and projected into stratum radiatum of CA3/4 and CA1 as well as stratum pyramidale of CA3. Like the dendrites of type I cells, type II interneurones often possessed varicosities (panels *C* and *D*). Scale bar in panel *D*, 25 μm (applies to all panels).

mEPSCs on CA3 pyramids (McBain & Dingledine, 1992), miniature GABAergic IPSCs on dentate granule cells (Edwards *et al.* 1990) and EPSCs on hilar interneurones (Livsey & Vicini, 1992). The lack of correlation between the amplitude and rise time (Fig. 7*C*) indicates that filtering is not the only determinant of the mEPSC amplitude. Recently, Raastad, Storm & Andersen (1992) concluded that the

variability in amplitude of single fibre EPSCs received by CA1 pyramidal neurones is not adequately described by dendritic filtering of the synaptic current and is more likely to be explained by variability in quantal synaptic transmission. Possible explanations include a variable quantal content (Bekkers & Stevens, 1990) or a mechanism that 'boosts' the response of more distal synapses (Redman & Walmsley, 1983).

Morphology of stratum radiatum interneurones

Intracellular injection of biocytin or the fluorescent dye Lucifer Yellow permitted *post hoc* morphological identification of stratum radiatum interneurones following whole-cell recording. Although the morphologies of these interneurones were quite divergent, most cells shared common features (Fig. 8). Whereas stratum radiatum interneurones could be distinguished by pharmacological and kinetic properties (see above for details) the morphologies of types I and II cells were not strikingly different and it was impossible to characterize these cells based on morphology alone.

Interneurones did not possess morphologies characteristic of pyramidal neurones or either stellate or basket interneurones but were reminiscent of the 'short axon' cells of radiatum described by Lorente de Nò (1934) and later by Lang & Frotscher (1990). The cell bodies of these cells were usually 20–40 μm in diameter. These cells had four to six divergent dendritic processes which often projected radially from the cell body for several hundred micrometres (Fig. 8*A* and *B*). The dendritic orientation of these cells was highly variable. Dendrites typically ramified and terminated throughout stratum radiatum and pyramidale (Fig. 8*A* and *B*), sometimes extending into the molecular layer and hilus of the dentate gyrus (Fig. 8*C* and *D*). Dendrites often possessed numerous swellings or varicosities thought to be characteristic of dendritic growth (e.g. Fig. 8*B*, *C* and *D*) (Schlander & Frotscher, 1986).

DISCUSSION

Heterogeneity in excitatory synaptic receptors

These results can be most easily explained if one assumes that the spontaneous mEPSCs received by type I and type II interneurones are mediated by different glutamate receptors. The difference between types I and II interneurones in the shape of their kainate *I–V* relations might be accounted for by the presence of edited GluR2 subunits in the AMPA receptors of type I but not type II cells. Of the known glutamate receptor subunits, only GluR1, GluR3, GluR4 or their combinations (Boulter *et al.* 1990; Nakanishi *et al.* 1990), and GluR6(Q621) (Dingledine, Hume & Heinemann, 1992), form strong inwardly rectifying receptor channels. Co-assembly of these glutamate receptor subunits with edited (Sommer, Kohler, Sprengel & Seeburg, 1991) GluR2 subunits converts the *I–V* relation from inwardly rectifying to linear or modestly outwardly rectifying (Boulter *et al.* 1990; Sakimura *et al.* 1990; Nakanishi *et al.* 1990; Hume, Dingledine & Heinemann, 1991; Verdoorn, Burnashev, Monyer, Seeburg & Sakmann, 1991). It is unlikely that GluR6 contributes to inward rectification in type II cells since the EC_{50} of kainate is approximately 1 μM in homomeric GluR6(R621) receptors (Egebjerg, Bettler, Hermans-Borgmeyer & Heinemann, 1991), whereas in this study 100 μM kainate did not produce a maximum response in type II cells (data not shown).

Miniature EPSCs on type I interneurones, like CA3 pyramidal neurones (McBain & Dingledine, 1992), CA1 pyramidal neurones (Hestrin *et al.* 1990), CA1 interneurones (Sah *et al.* 1990) and cultured hippocampal neurones (Bekkers & Stevens, 1990), are mediated by AMPA and NMDA receptors co-localized at the same synapse. The majority of type II interneurones seem to possess AMPA receptors capable of passing current only at negative membrane potentials, however, and most of these cells appeared to be devoid of synaptic NMDA receptors. Iino and co-workers have described an as yet unidentified small 'elliptical' hippocampal neurone in culture which they termed a 'type II' cell, whose *I–V* relation shows some degree of inward rectification. The kainate-activated receptors on these cells showed high calcium permeability (Iino *et al.* 1990; Ozawa *et al.* 1991). It is possible that the cell type described by Iino *et al.* (1990) is the stratum radiatum type II interneurone described in this study. However, in contrast to the cell type described by Iino *et al.* (1990) many of our type II interneurones did not show any outward current at potentials up to +60 mV.

Kainate currents and mEPSCs on both type I and type II interneurones are blocked by CNQX, indicating postsynaptic receptors of the AMPA type on both interneurones. It is necessary to consider whether very poor voltage control could account for the observed inward rectification in type II cells. It is clear that voltage control is not maintained well over distal regions of either type I or type II interneurone (Fig. 7*A* and *B*), as is the case for CA3 pyramidal neurones (McBain & Dingledine, 1992). We do not think this explanation adequate to account for the difference between type I and type II cells, however. The series resistance was approximately equal for recordings from both cell types ($25 \pm 1{\cdot}4$ MΩ in 25 type I cells, and $18 \pm 3{\cdot}9$ MΩ in 7 type II cells). Moreover, inadequate voltage clamp does not manifest itself as strong inward rectification when the membrane *I–V* relation is nearly linear. Indeed, in several type I cells with poor input resistance (< 100 MΩ) and therefore probably poor voltage control, the observed reversal potential of kainate currents was very positive (> 25 mV), yet the *I–V* relation was still nearly linear. None of these cells has been included in this paper. We conclude that the observed inward rectification in type II interneurones is more likely to be a property of the AMPA receptors themselves. Indeed, inwardly rectifying current–voltage relations to kainate have also been observed in outside-out patches pulled from stratum radiatum interneurones (J. C. McBain & R. Dingledine, unpublished observations).

Kinetics of mEPSCs on interneurones and pyramidal cells

Interneurones and pyramidal cells located within the CA1 region display EPSCs with apparently identical kinetics and *I–V* relations, despite different morphologies (Sah *et al.* 1990). As shown in Table 1 and Figs 3–6, this is not the case in the CA3 region. The electrotonic length of type I interneurones is similar to that of CA3 pyramidal cells, but the observed differences in mEPSC kinetics between these two cell types might be explained partly by differences in the location of excitatory synapses. Livsey & Vicini (1992) reported that EPSC kinetics on hilar interneurones that lacked spines were faster than those with numerous spines. Dendritic spines on type I (or type II) interneurones were not prominent, although no systematic study was undertaken.

Differences in glutamate receptor subunit expression may also contribute to the different mEPSC kinetics in CA3 pyramidal neurones and type I interneurones. Within the CA3 region the expression of the flop splice variants of glutamate receptor subunits are confined to non-pyramidal cells (Monyer *et al.* 1991), whereas CA3 pyramidal neurones express only the flip splice variants. Receptors assembled from flop-containing subunits may desensitize more slowly in response to glutamate than those expressing flip (Sommer *et al.* 1990). Although indirect, these observations are consistent with faster EPSC kinetics in type I interneurones. A better understanding of the observed differences in *I–V* relations and mEPSC kinetics in the different neurone types awaits a genetic analysis of individual, physiologically characterized neurones.

Possible functions of excitatory inputs to type II cells

It is unlikely that rectification *per se* has a significant physiological role in these cells, but calcium flux through receptor channels may be substantial. A prominant feature of receptors assembled from any combination of native or mutant glutamate receptor subunits that exhibit inward rectification, is that calcium permeability is high (Hollmann, Hartley & Heinemann, 1991; Hume *et al.* 1991; Burnashev, Monyer, Seeburg & Sakmann, 1992; Dingledine *et al.* 1992). We propose that type II interneurones may utilize AMPA receptors that permit high calcium influx to compensate for the lack of synaptic NMDA receptors. A direct test of this hypothesis requires measurement of the calcium permeability of glutamate receptors on type II interneurones. Although we have not tested Ca^{2+} permeability directly, in two cells substitution of 60 mM $BaCl_2$ for 130 mM NaCl in the perfusion solution caused a large reduction of the kainate current at -80 mV without changing the basic shape of the inwardly rectifying *I–V* relation (not shown). This is consistent with findings from the cloned glutamate receptor subunits (Hume *et al.* 1991; Dingledine *et al.* 1992).

Calcium-permeable AMPA receptors would permit substantial postsynaptic calcium influx without the necessity for the prior depolarization needed by NMDA receptors. Thus selection of NMDA or type II AMPA receptors would allow neurones control over the range of membrane potentials at which excitatory synaptic inputs result in significant calcium influx. Calcium-permeable AMPA receptors could also endow neurones with the potential for synaptic plasticity without the need for postsynaptic activation of NMDA receptors, as occurs for long-term potentiation of mossy fibre synapses onto CA3 pyramidal neurones (Zalutsky & Nicoll, 1990), which possess few NMDA receptors (Monaghan & Cotman, 1985). We are unaware of studies of synaptic plasticity in CA3 interneurones, although interneurones in the CA1 region participate in long-term potentiation (Taube & Schwartzkroin, 1987).

The origin(s) of the presynaptic terminals making synapses with type II interneurones is at present unknown. The two most likely inputs are mossy fibres from dentate granule cells and recurrent collaterals from CA3 pyramidal neurones. Mossy fibres form asymmetric excitatory synapses with some CA3 stratum radiatum interneurones, suggesting a role for these cells in feedforward inhibition and control of pyramidal cell excitability (Frotscher, 1985). The AMPA receptor component of mossy fibre synapses (Brown & Johnston, 1983) exhibits a linear *I–V* relation in contrast to type II interneurones. To our knowledge there has been no previous report of AMPA receptor-mediated synaptic currents in the hippocampal structure

which show such strong inward rectification as seen in type II interneurones. Further work is required to elucidate the physiological function of these synaptic currents and the origins of the presynaptic terminals innervating them.

We would like to thank Dr Steve Traynelis for generously supplying the data analysis software, Tracy Brown for help with the biocytin staining and Dr J. C. Lacaille for helpful comments. This work was supported by NIH grant NS17771, Bristol-Myers Squibb Co. and the Klingenstein Foundation.

REFERENCES

ANDERSEN, P. (1975). Organization of hippocampal neurons and their interconnections. In *The Hippocampus*, vol. I, ed. ISAACSON, R. L. & PRIBAM, K. H., pp. 155–175. Plenum Press, New York.

BEKKERS, J. M. & STEVENS, C. F. (1989). NMDA and non-NMDA receptors are co-localized at individual excitatory synapses in cultured rat hippocampus. *Nature* **341**, 230–233.

BOULTER, J., HOLLMANN, M., O'SHEA-GREENFIELD, A., HARTLEY, M., DENERIS, E., MARON, C. & HEINEMANN, S. (1990). Molecular cloning and functional expression of glutamate receptor subunit genes. *Science* **249**, 1033–1037.

BROWN, T. H. & JOHNSTON, D. (1983). Voltage-clamp analysis of mossy fiber synaptic input to hippocampal neurons. *Journal of Neurophysiology* **50**, 487–507.

BURNASHEV, N., MONYER, H., SEEBURG, P. H. & SAKMANN, B. (1992). Divalent ion permeability of AMPA receptor channels is dominated by the edited form of a single subunit. *Neuron* **8**, 189–198.

BUZSAKI, G. & EIDELBERG, E. (1982). Direct afferent excitation and long-term potentiation of hippocampal interneurons. *Journal of Neurophysiology* **48**, 597–607.

DINGLEDINE, R., HUME, R. I. & HEINEMANN, S. F. (1992). Structural determinants of barium permeation and rectification in non-NMDA glutamate receptor channels. *Journal of Neuroscience* **12**, 4080–4087.

EDWARDS, F. A., KONNERTH, A., SAKMANN, B. & TAKAHASHI, T. A. (1989). A thin slice preparation for patch clamp recordings from neurones of mammalian central nervous system. *Pflügers Archiv* **430**, 600–612.

EGEBJERG, J., BETTLER, N., HERMANS-BORGMEYER, I. & HEINEMANN, S. (1991). Cloning of a cDNA for a glutamate receptor subunit activated by kainate but not AMPA. *Nature* **351**, 745–748.

FROTSCHER, M. (1985). Mossy fibres form synapses with identified pyramidal basket cells in the CA3 region of the guinea-pig hippocampus: a combined Golgi-electron microscope study. *Journal of Neurocytology* **14**, 245–259.

FROTSCHER, M., LERANTH, C. S., LUBBERS, K. & OERTEL, W. H. (1984). Commissural afferents innervate glutamate decarboxylase immunoreactive non-pyramidal neurons in the guinea pig hippocampus. *Neuroscience Letters* **46**, 137–143.

FROTSCHER, M. & ZIMMER, J. (1983). Commissural fibers terminate on non-pyramidal neurons in the guinea pig hippocampus – a combined Golgi/EM degeneration study. *Brain Research* **265**, 289–293.

HAMILL, O. P., MARTY, A., NEHER, E., SAKMANN, B. & SIGWORTH, F. J. (1981). Improved patch-clamp techniques for high-resolution current recording from cells and cell-free membrane patches. *Pflügers Archiv* **391**, 85–100.

HESTRIN, S., NICOLL, R. A., PERKEL, D. J. & SAH, P. (1990). Analysis of excitatory synaptic action in pyramidal cells using whole-cell recording from rat hippocampal slices. *Journal of Physiology* **422**, 203–225.

HOLLMANN, M., HARTLEY, M. & HEINEMANN, S. (1991). Ca^{2+} permeability of KA–AMPA-gated glutamate receptor channels depends on subunit composition. *Science* **252**, 643–648.

HUME, R. I., DINGLEDINE, R. & HEINEMANN, S. F. (1991). Identification of a site in glutamate receptor subunits that controls calcium permeability. *Science* **253**, 1028–1032.

IINO, M., OZAWA, S. & TSUZUKI, K. (1990). Permeation of calcium through excitatory amino acid receptor channels in cultured rat hippocampal neurones. *Journal of Physiology* **424**, 151–165.

JOHNSTON, D. & BROWN, T. H. (1983). Interpretation of voltage-clamp measurements in hippocampal neurons. *Journal of Neurophysiology* **50**, 464–486.

KEINANEN, K., WISEN, W., SOMMER, B., WERNER, P., HERB, A., VERDOORN, T. A., SAKMANN, B. & SEEBURG, P. H. (1990). A family of AMPA-selective glutamate receptors. *Science* **249**, 556–560.

KISVARDAY, Z. F., MARTIN, K. A. C., FREUND, T. F., MAGLOCZKY, Z. S., WHITTERIDGE, D. & SOMOGYI, P. (1986). Synaptic targets of HRP-filled layer III pyramidal cells in the cat striate cortex. *Experimental Brain Research* **64**, 541–552.

LANG, U. & FROTSCHER, M. (1990). Postnatal development of nonpyramidal neurons in the rat hippocampus (areas CA1 and CA3): a combined Golgi electron microscope study. *Anatomy and Embryology* **181**, 533–545.

LIVSEY, C. T. & VICINI, S. (1992). Slower spontaneous excitatory postsynaptic currents in spiny versus aspiny hilar neurons. *Neuron* **8**, 1–20.

LORENTE DE NÒ, R. (1934). Studies on the structure of the cerebral cortex. II. Continuation of the study of the ammonic system. *Journal of Psychology and Neurology* (Leipzig) **46**, 113–177.

LOY, R. (1980). Development of afferent lamination in Ammon's horn of the rat. *Anatomy and Embryology* **159**, 257–275.

MCBAIN, C. J. & DINGLEDINE, R. (1991). Patch clamp recordings from interneurones of hippocampal subfield CA3; responses to excitatory amino acids. *Society for Neuroscience Abstracts* **17**, 259.

MCBAIN, C. J. & DINGLEDINE, R. (1992). Dual-component miniature excitatory synaptic currents in rat hippocampal CA3 pyramidal neurons. *Journal of Neurophysiology* **68**, 16–27.

MCBAIN, C. J., EATON, J. V., BROWN, T. & DINGLEDINE, R. (1992). CNQX increases spontaneous inhibitory input to CA3 pyramidal neurones in neonatal rat hippocampal slices. *Brain Research* **592**, 255–260.

MAYER, M. L. & WESTBROOK, G. L. (1987). The physiology of excitatory amino acids in the vertebrate central nervous system. *Progress in Neurobiology* **28**, 197–291.

MAYER, M. L., WESTBROOK, G. L. & GUTHRIE, P. B. (1984). Voltage-dependent block by Mg of NMDA responses in spinal cord neurones. *Nature* **309**, 261–263.

MILES, R. (1991). Synaptic excitation of inhibitory cells by single CA3 hippocampal pyramidal cells of the guinea-pig *in vitro*. *Journal of Physiology* **428**, 61–77.

MILES, R. & WONG, R. K. S. (1984). Unitary inhibitory synaptic potentials in the guinea-pig hippocampus *in vitro*. *Journal of Physiology* **356**, 97–113.

MILES, R. & WONG, R. K. S. (1987). Inhibitory control of local excitatory circuits in the guinea-pig hippocampus. *Journal of Physiology* **388**, 611–629.

MONAGHAN, T. & COTMAN, C. W. (1985). Two classes of *N*-methyl-D-aspartate-sensitive L-[^{3}H]glutamate binding sites in the rat brain. *Journal of Neuroscience* **5**, 2909–2919.

MONYER, H., SEEBURG, P. H. & WISDEN, W. (1991). Glutamate-operated channels: developmentally early and mature forms arise by alternative splicing. *Neuron* **6**, 799–810.

NAKANISHI, N., SHNEIDER, N. A. & AXEL, R. (1990). A family of glutamate receptor genes: Evidence for the formation of heteromultimeric receptors with distinct channel properties. *Neuron* **5**, 569–581.

NOWAK, L., BREGESTOVSKI, P., ASCHER, P., HERBET, A. & PROCHIANTZ, A. (1984). Magnesium gates glutamate-activated channels in mouse central neurones. *Nature* **307**, 462–465.

OZAWA, S., IINO, M. & TSUZUKI, K. (1991). Two types of kainate response in cultured rat hippocampal neurons. *Journal of Neurophysiology* **66**, 2–11.

RAASTAD, M., STORM, J. F. & ANDERSEN, P. (1992). Putative single quantum and single fibre excitatory postsynaptic currents show similar amplitude range and variability in rat hippocampal slices. *European Journal of Neuroscience* **4**, 113–117.

RALL, W. (1969). Time constants and electrotonic length of membrane cylinders and neurons. *Biophysical Journal* **9**, 1483–1508.

RAMON, Y, CAJAL, S. (1968). *The Structure of Ammon's Horn*. C. C. Thomas, Springfield, IL, USA.

REDMAN, S. & WALMSLEY, B. (1983). The time course of synaptic potentials evoked in cat spinal motoneurones at identified group Ia synapses. *Journal of Physiology* **343**, 117–133.

RIBAK, C. E., VAUGHN, J. E. & BARBER, R. P. (1981). Immunocytochemical localization of GABAergic neurones at the electron microscopical level. *Histochemical Journal* **13**, 555–582.

RIBAK, C. E., VAUGHN, J. E. & SAITO, K. (1978). Immunocytochemical localization of glutamic acid decarboxylase in neuronal somata following colchicine inhibition of axonal transport. *Brain Research* **140**, 315.

SAH, P., HESTRIN, S. & NICOLL, R. A. (1989). Tonic activation of NMDA receptors by ambient glutamate enhances excitability of neurons. *Science* **246**, 815–246.

SAH, P., HESTRIN, S. & NICOLL, R. A. (1990). Properties of excitatory postsynaptic currents recorded *in vitro* from rat hippocampal interneurones. *Journal of Physiology* **430**, 605–616.

SAKIMURA, K., BUJO, H., KUSHIYA, E., ARAKI, K., YAMAZAKI, M., MEGURO, H., WARASHINA, A., NUMA, S. & MISHINA, M. (1990). Functional expression from cloned cDNAs of glutamate receptor species responsive to kainate and quisqualate. *FEBS Letters* **272**, 73–80.

SCHLANDER, M. & FROTSCHER, M. (1986). Non-pyramidal neurons in the guinea pig hippocampus (a combined Golgi–electron microscope study). *Anatomy and Embryology* **174**, 35–47.

SCHWARTZKROIN, P. A. & KUNKEL, D. D. (1985). Morphology of identified interneurons in the CA1 regions of guinea pig hippocampus. *Journal of Comparative Neurology* **232**, 205–218.

SERESS, L. & RIBAK, C. E. (1985). A combined Golgi–electron microscopic study of non-pyramidal neurons in the CA1 area of the hippocampus. *Journal of Neurocytology* **14**, 717–730.

SOMMER, B., KEINANEN, K., VERDOORN, T. A., WISDEN, W., BURNASHEV, N., HERB, A., KOHLER, M., TAKAGI, T., SAKMANN, B. & SEEBURG, P. H. (1990). Flip and flop: A cell-specific functional switch in glutamate-operated channels of the CNS. *Science* **249**, 1580–1585.

SOMMER, B., KOHLER, M., SPRENGEL, R. & SEEBURG, P. H. (1991). RNA editing in brain controls a determinant of ion flow in glutamate-gated channels. *Cell* **67**, 11–19.

SOMOGYI, P., SMITH, A. D., NUNZI, M. G., GORIO, A., TAKAGI, H. & WU, J. Y. (1983). Glutamate decarboxylase immunoreactivity in the hippocampus of the cat: distribution of immunoreactive synaptic terminals with special reference to the axon initial segment of pyramidal neurons. *Journal of Neuroscience* **3**, 1450–1468.

STORM-MATHISEN, J., LEKNES, A. K., BORE, A. T., VAALAND, J. L., EDMINSON, P., HAUG, F. M. S. & OTTERSEN, O. P. (1983). First visualisation of glutamate and GABA in neurones by immunocytochemistry. *Nature* **301**, 517–520.

SWANN, J. W., BRADY, R. J. & MARTIN, D. L. (1989). Postnatal development of GABA-mediated synaptic inhibition in rat hippocampus. *Neuroscience* **28**, 551–561.

TAUBE, J. S. & SCHWARTZKROIN, P. A. (1987). Intracellular recording from hippocampal CA1 interneurons before and after development of long-term potentiation. *Brain Research* **419**, 32–36.

TRAUB, R. D., MILES, R., WONG, R. K. S., SCHULMAN, L. S. & SCHNEIDERMAN, J. H. (1987). Models of synchronized hippocampal bursts in the presence of inhibition. II. Ongoing spontaneous population events. *Journal of Neurophysiology* **58**, 752–764.

VERDOORN, T. A., BURNASHEV, N., MONYER, H., SEEBURG, P. H. & SAKMANN, B. (1991). Structural determinants of ion flow through recombinant glutamate receptor channels. *Science* **252**, 1715–1718.

WERNER, P., VOIGT, M., KEINANEN, K., WISDEN, W. & SEEBURG, P. H. (1991). Cloning of a putative high-affinity kainate receptor expressed predominantly in hippocampal CA3 cells. *Nature* **351**, 742–744.

ZALUTSKY, R. A. & NICOLL, R. A. (1990). Comparison of two forms of long-term potentiation in single hippocampal neurons. *Science* **248**, 1619–1624.